Optical properties of atmospheric constituents

Direct effects of aerosols optical properties on climate

Scattering Aerosols

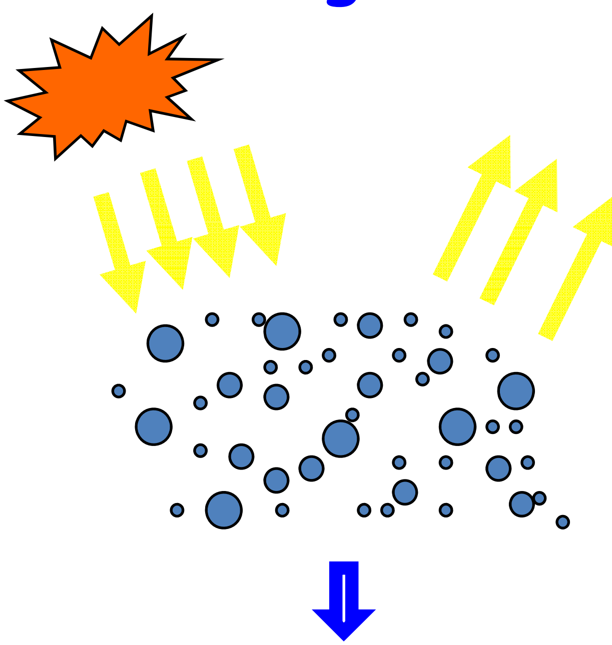

Cooling

Absorbing Aerosols

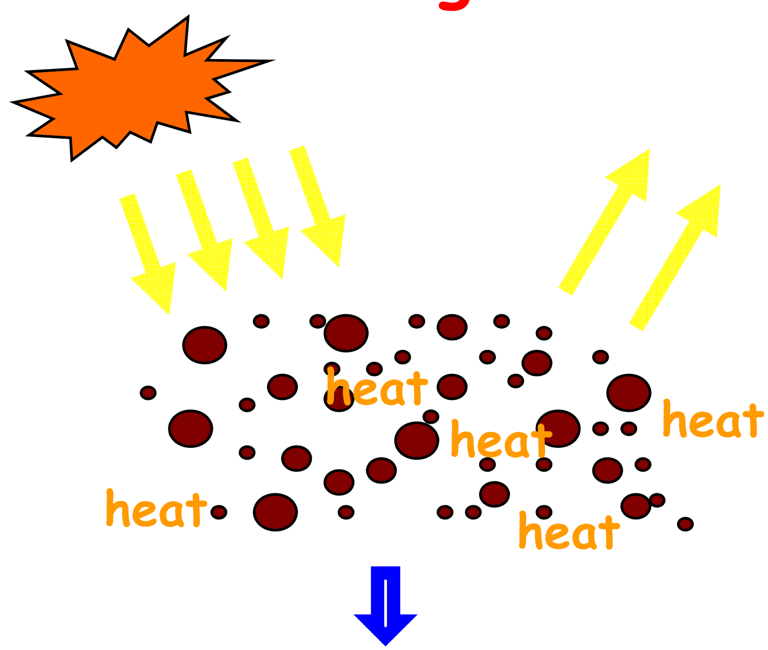

Clouds evaporation

Graphics: Yinon Rudich

KRILL PRIZES

FOR EXCELLENCE IN SCIENTIFIC RESEARCH

Krill Prizes for Excellence in Scientific Research are awarded in Honor and in Memory of BENJAMIN AND GITLA KRILL MANSBACH SHLANGER.

Six Krill Prizes, of $10,000 each, are awarded annually, in Exact Sciences, Life Sciences, Medicine, Agriculture and Engineering, to excelling faculty members at the Universities in Israel, who hold the untenured positions of Lecturer, or Senior Lecturer.

Recipients are selected by the Wolf Foundation Scholarship Committee, from among outstanding candidates, submitted by all Israeli Universities. The selection is made on the basis of the candidate´s excellence and the importance of his or her field of research.

Climatic effects of aerosols: Large uncertainties

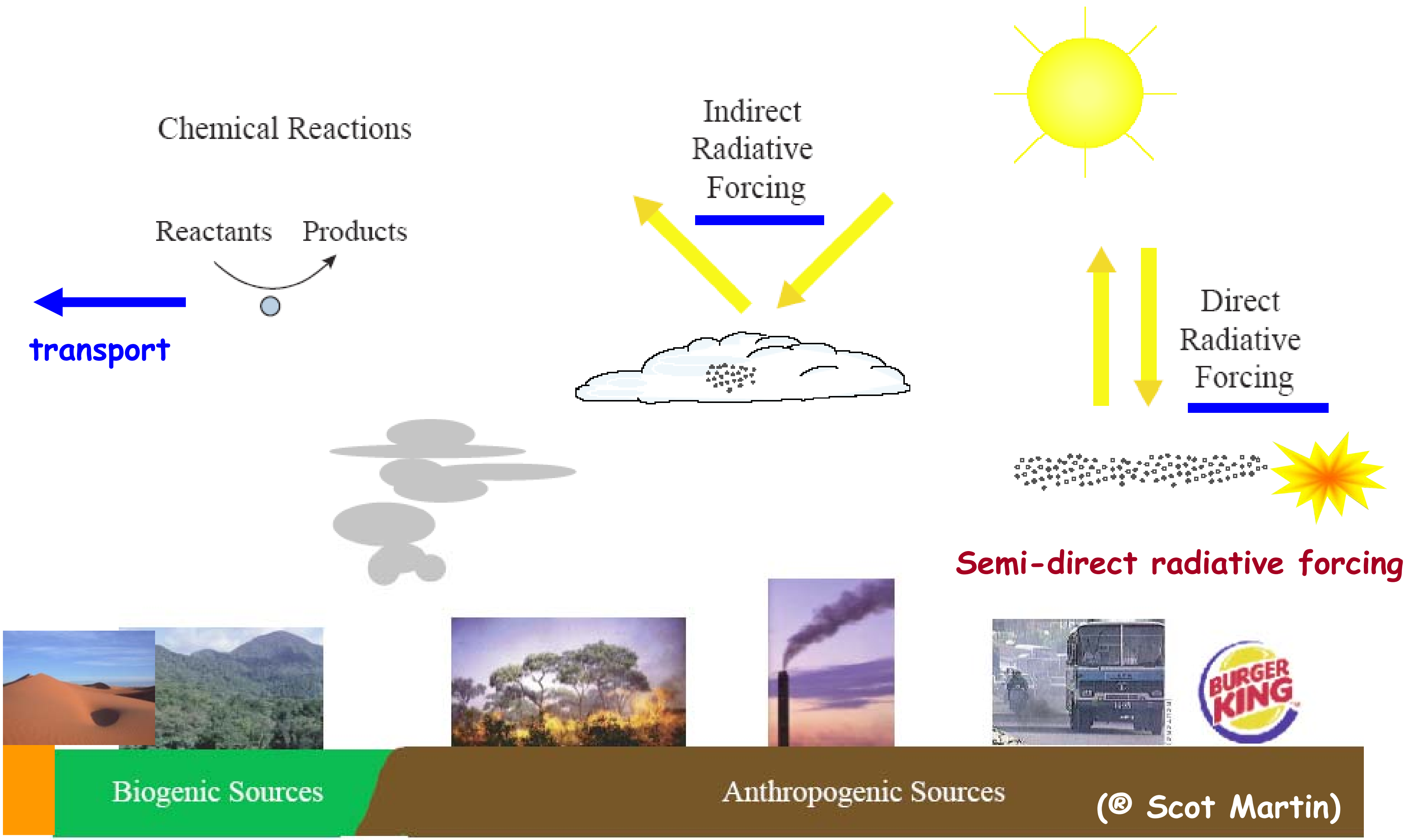

Optically important Aeroslos in the atmosphere

- Air molecules
- Black carbon aerosols
- Soil dust aerosols
- Organic aerosols
- Aerosols of marine origin
- H_2O

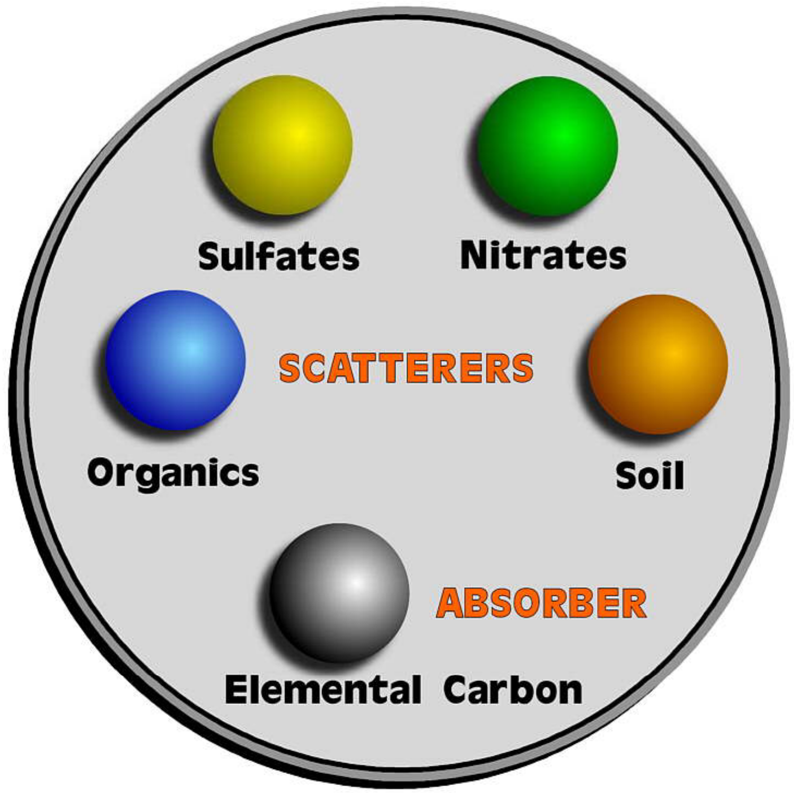

*vista.cira.colostate.edu/improve/Education/Workshops/WESTAR/Malm/**partii_malm**.ppt*

Different approaches to study aerosols OP:

1. Lab (isolated, possibly modified)

2. Inversion of in-situ measurements (no control, hard to isolate specific contributions)

Aerosols science is extremely complex due to wide variety of different types and aging effects.

Scattering and absorption cross-sections of aerosols:

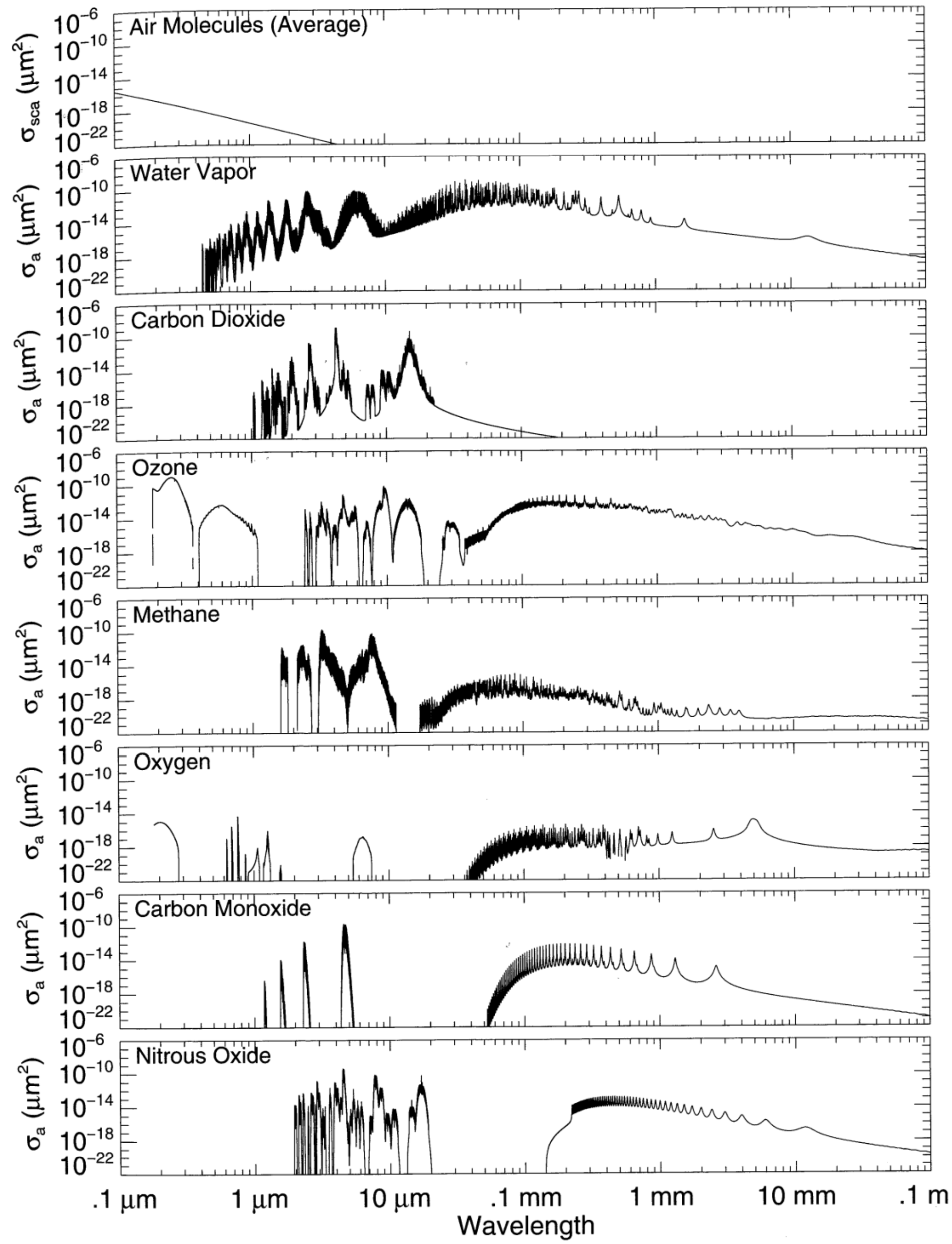

Figure 2.12: Absorption cross sections for most of the strongly absorbing atmospheric gases (1013 mb and 294 K) and average scattering cross section for air molecules (top panel).

Bohren and Clothaux, 2006.

Absorption lines are broadened by:
Doppler (motion of molecules and source of photons) $\propto$T

Self broadening (consequence of inter-molecular forces) $\propto$T

Foreign broadening (interactions with other molecules) $\propto$pressure, T

→ Expect absorption spectra to vary with Pressure and Temperature in the atmosphere.

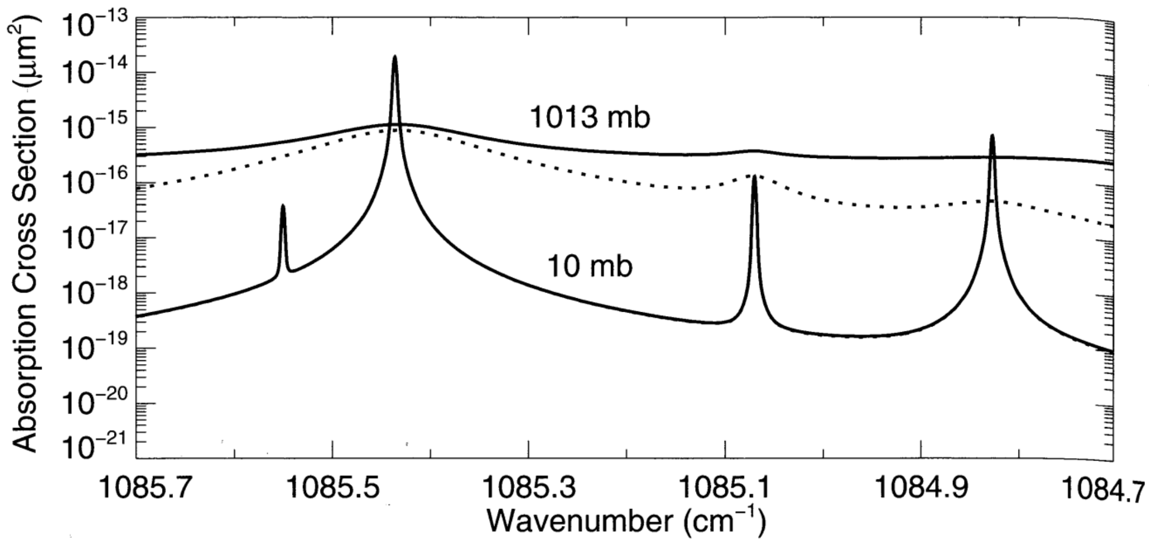

Figure 2.19: Line-by-line calculations of water vapor absorption at two pressure altitudes. The dashed curve shows a calculation from which continuum absorption is omitted. At 10 mb, omission of the continuum results in a curve indistinguishable from that shown.

Bohren and Clothaux, 2006.

Note: wavenumber=1/wavelength=ν/c

Effect of size of drops on scattering properties of cloud:

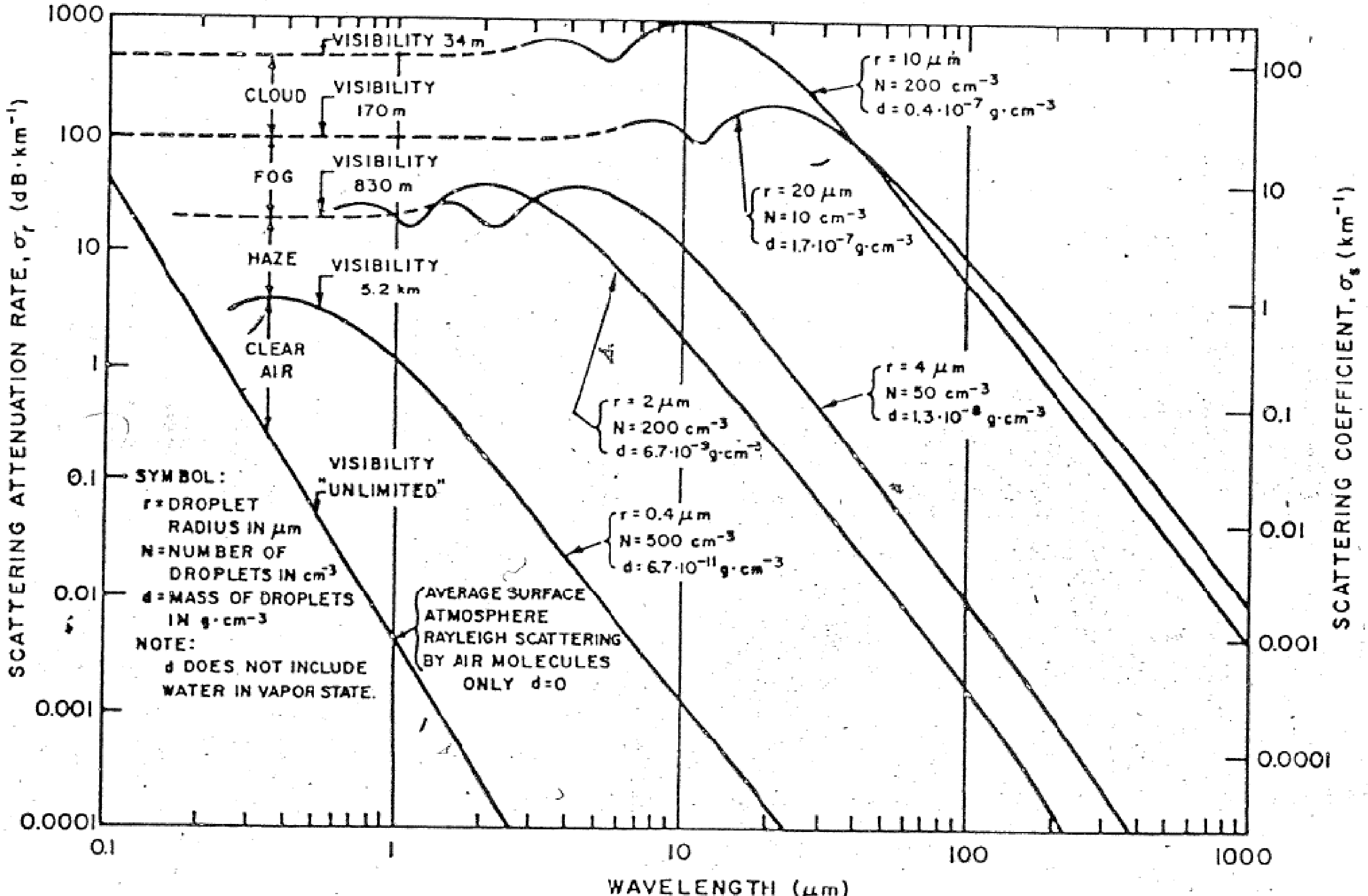

From Kopeika, 2002

Example: Mie output for a black carbon aerosol (sensitivity to size for the same composition)

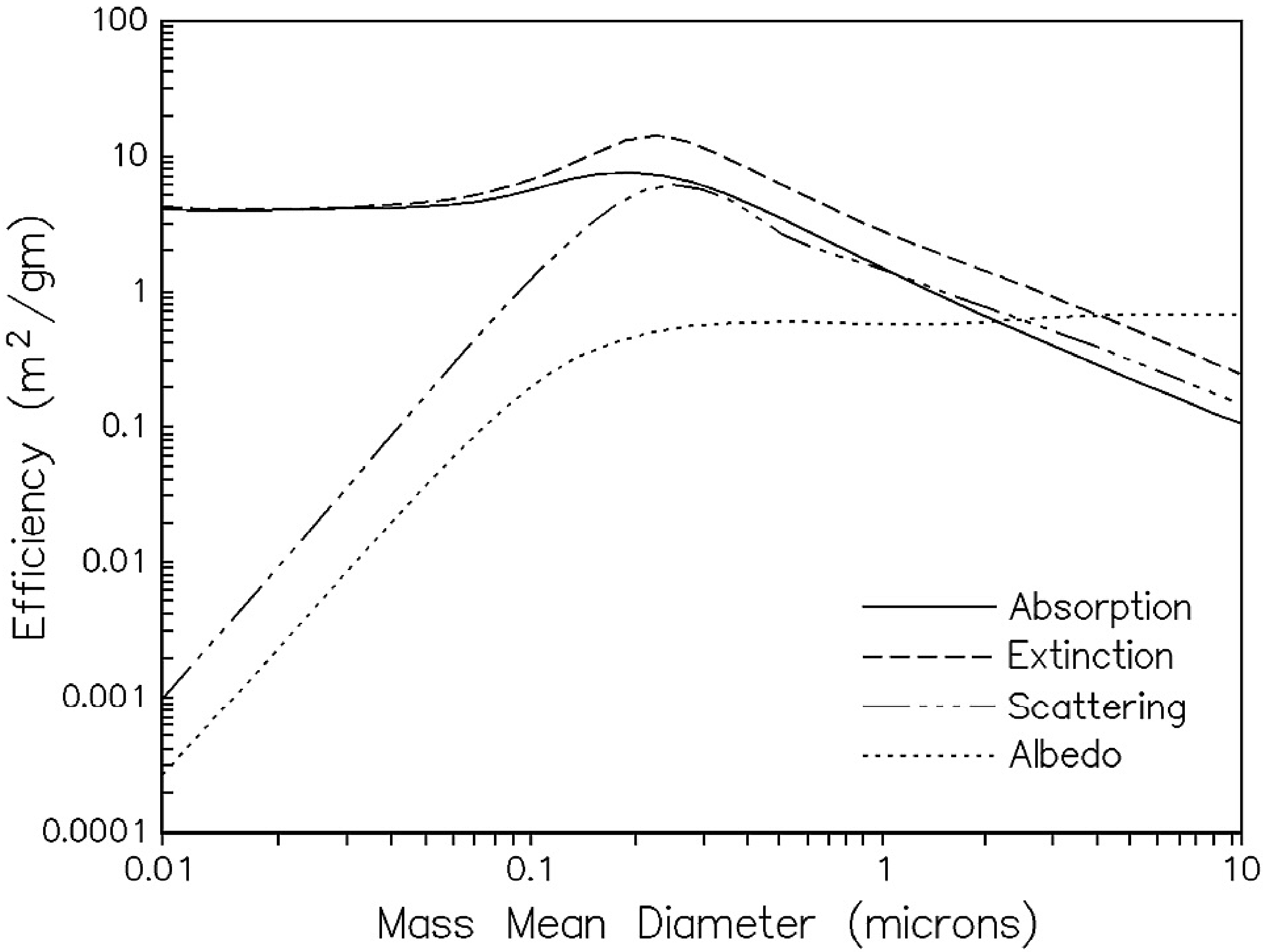

*vista.cira.colostate.edu/improve/Education/Workshops/WESTAR/Malm/**partii_malm**.ppt*

Light scattering experiment

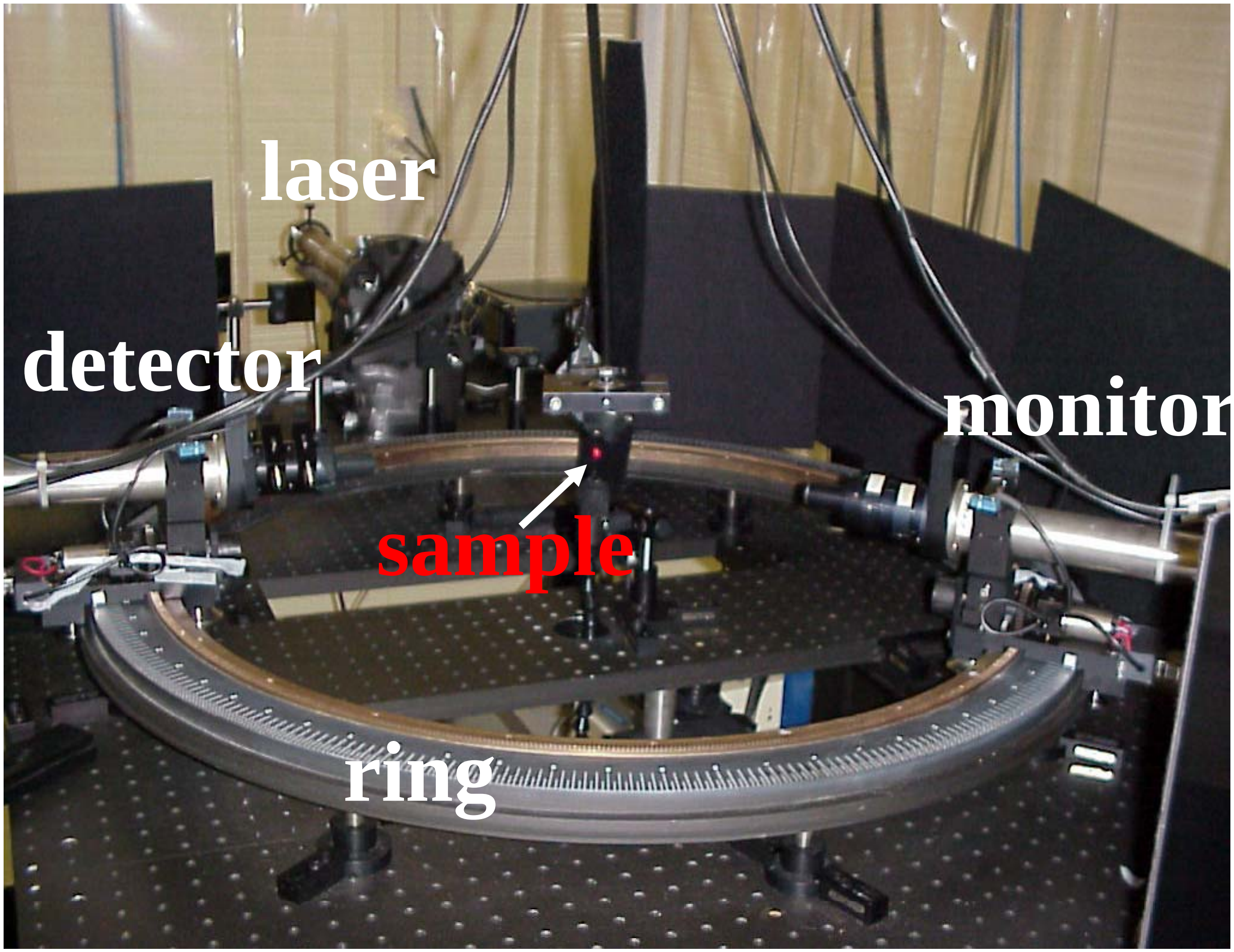

From presentation by Volten

Facts and Figures

name of sample	feldspar
origin	crushed piece of Feldspar rock from Finland
main constituents	K-feldspar, plagioclase, quartz
particle size	distributions measured with laser diffraction r_{eff}=1.0 micrometer, v_{eff} =1.0
particle shape	irregular (SEM image)
refractive index	estimated to be in the range: 1.5-1.6 - i0.001-0.00001
color	light pink to white powder
scattering matrix wavelength	from 5-173 degrees scattering angle 441.6 nm (figure) 632.8 nm (figure)
article	Scattering matrices of mineral particles at 441.6 nm and 632.8 nm. Volten H, Muñoz O, Rol E, de Haan JF, Vassen W, Hovenier JW, Muinonen K, Nousiainen T. Journal of Geophysical Research, 106, 17375-17401,2001

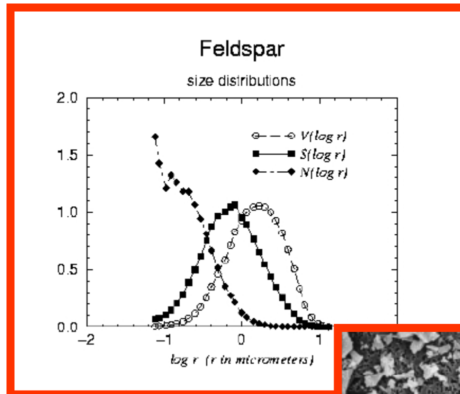

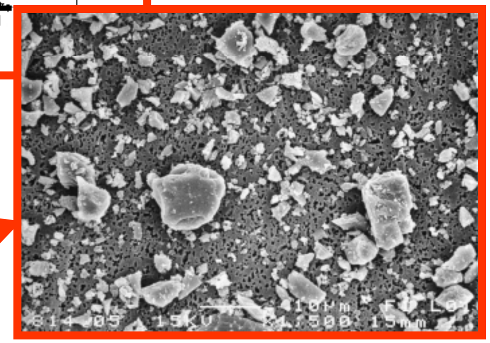

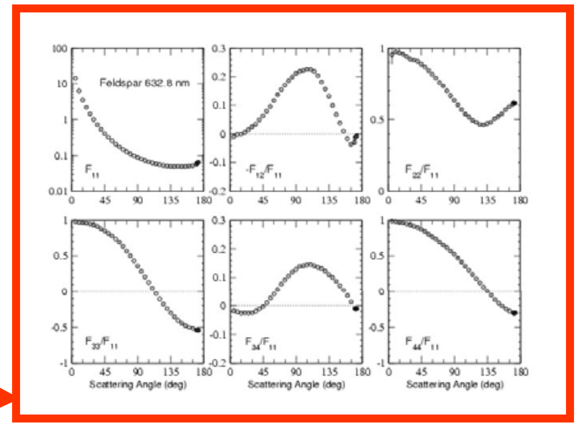

From presentation by Volten

Absorption by dust particles when suspended in water using an integrating sphere:

ID	Description	Origin	SPM (g m^{-3})	POC (g m^{-3})
ILL_1	Illite	Source Clay Minerals Repository, University of Missouri (ref. IMt-1)	37.71	
ILL_2	As above but different PSD	As above	26.53	0.86
KAO_1	Kaolinite (poorly crystallized)	As above, but ref. KGa-2	28.34	
KAO_2	As above but different PSD	As above	23.3	
MON_1	Ca-montmorillonite	As above, but ref. SAz-1	38.48	
MON_2	As above but different PSD	As above	28.52	0.73
CAL_1	Calcite	Natural crystal	26.48	
CAL_2	As above but different PSD	As above	12.60	
QUA_1	Quartz	Natural crystal	14.17	
SAH_1	Atmospheric dust from Sahara	Red rain event, Villefranche-sur-Mer, France, Nov 1996	43.43	1.28
SAH_2	As above but different PSD	As above	19.47	
AUS_1	Surface soil dust	Cliff shore, Palm Beach north of Sydney, Australia	32.03	0.87
AUS_2	As above but different PSD	As above	24.05	0.64
ICE_1	Ice-rafted particles	Glacier runoff, Kongsfjord, Spitsbergen, Norway	28.51	0.44
ICE_2	As above but different PSD	As above	22.37	
OAH_1	Surface soil dust	Oahu, Hawaii Islands	31.67	1.12
OAH_2	As above but different PSD	As above	18.05	0.62
KUW_1	Surface soil dust	Kuwait (eastern part, close to ocean)	23.36	
KUW_2	As above but different PSD	As above	23.10	6.27
NIG_1	Surface soil dust	Southwest Nigeria	37.06	2.71
SAN_1	Atmospheric dust	San Diego, California	17.08	2.73

Why did they suspend them in water?

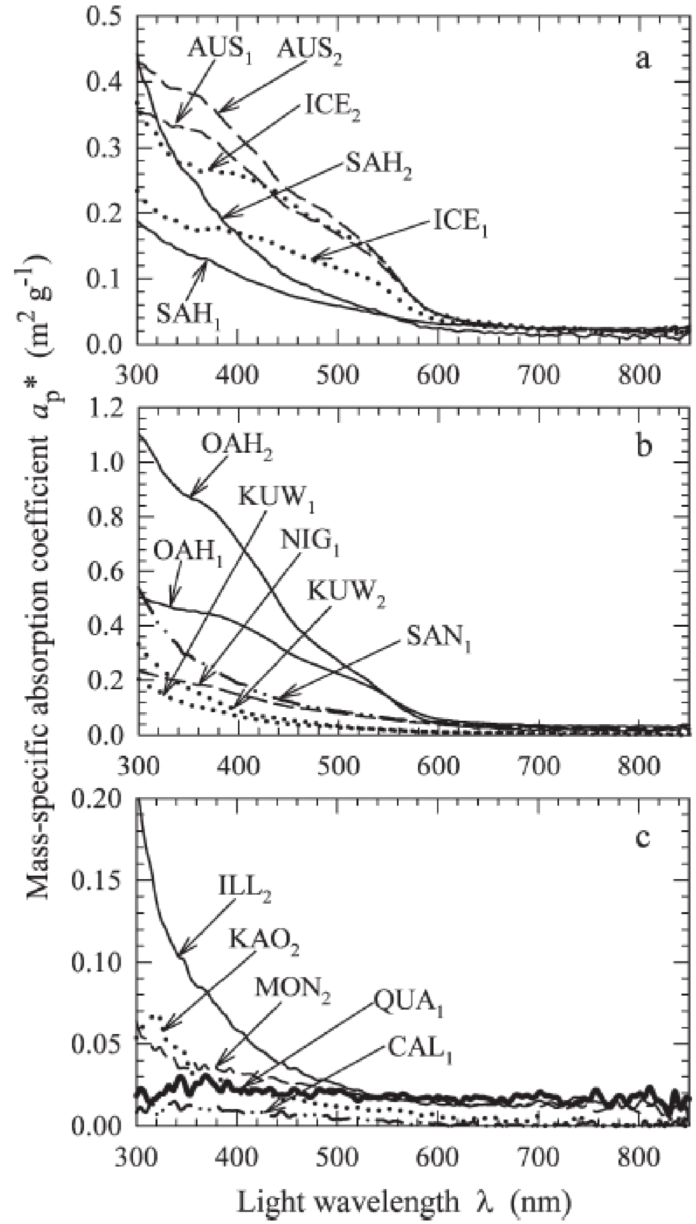

Fig. 3. (a, b) Spectra of mass-specific absorption coefficient of particles for samples of mixed particulate assemblages and (c) for samples of single-mineral species.

Stramski et al. 2007

Cavity ring down spectroscopy:

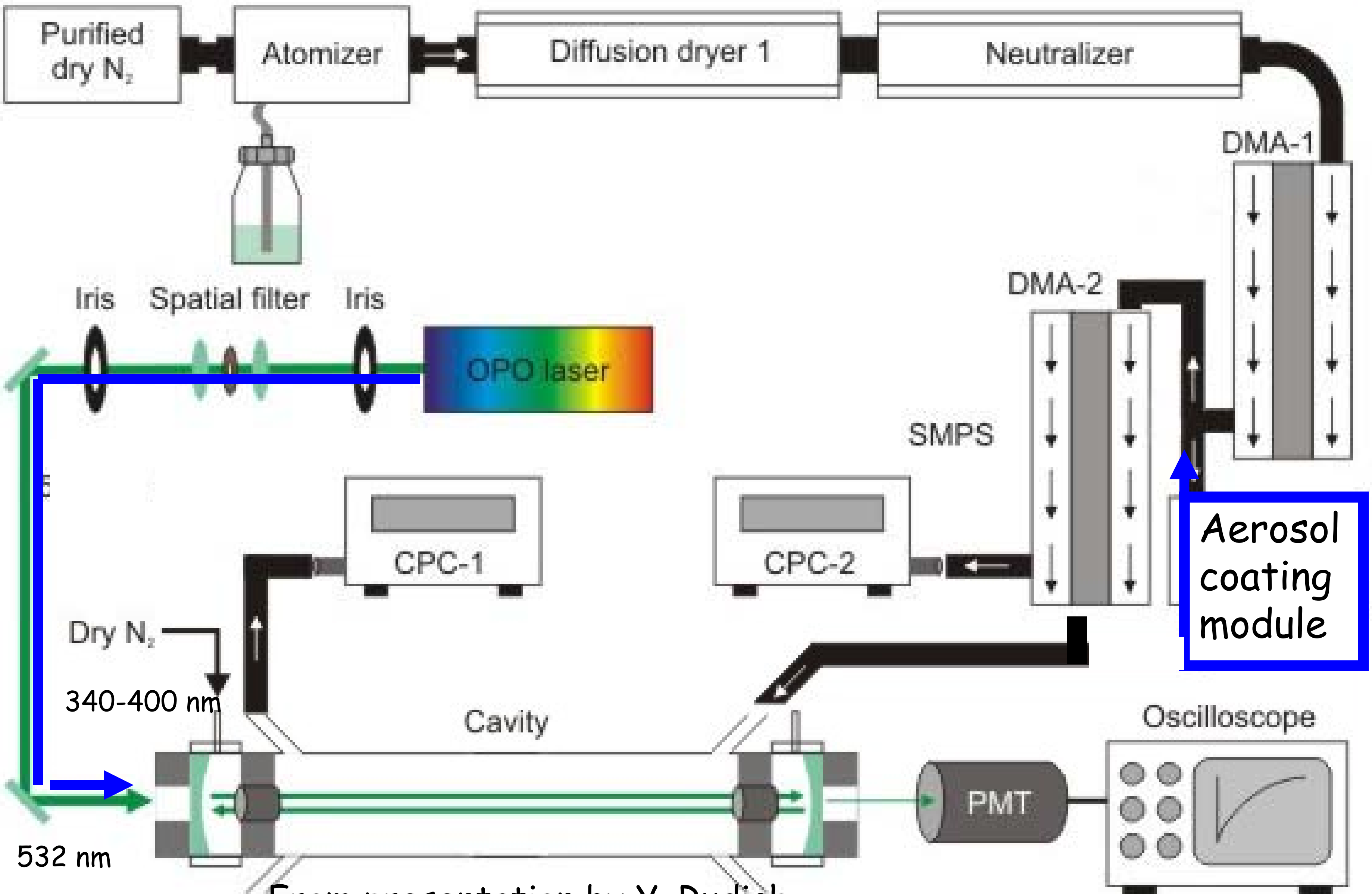

From presentation by Y. Rudich

Complex refractive index of single composition aerosol

Scattering only

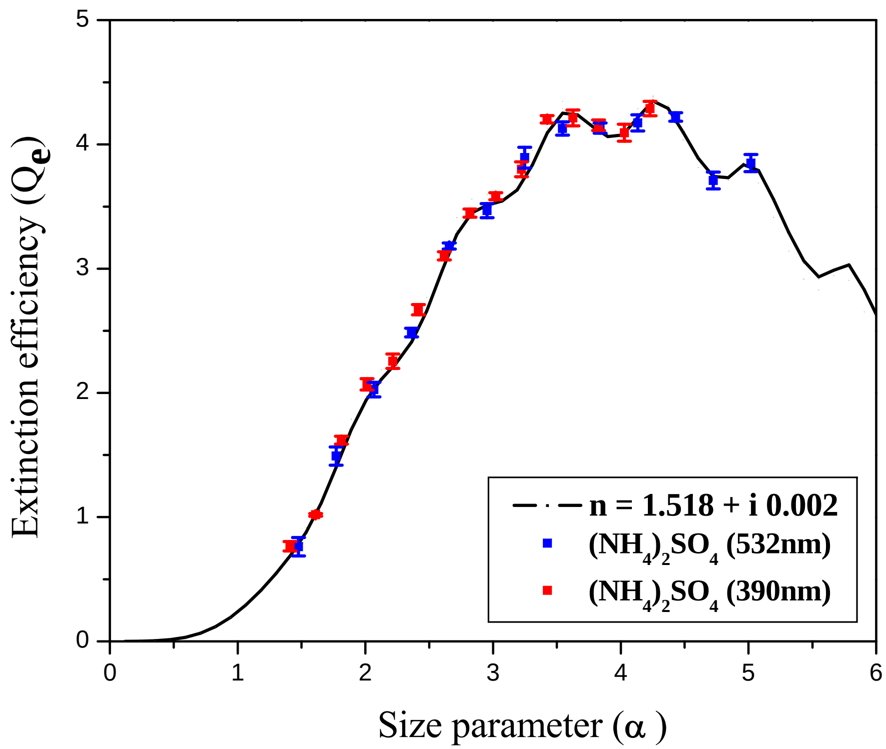

Abo Riziq, ACP 2006

Strongly absorbing aerosol

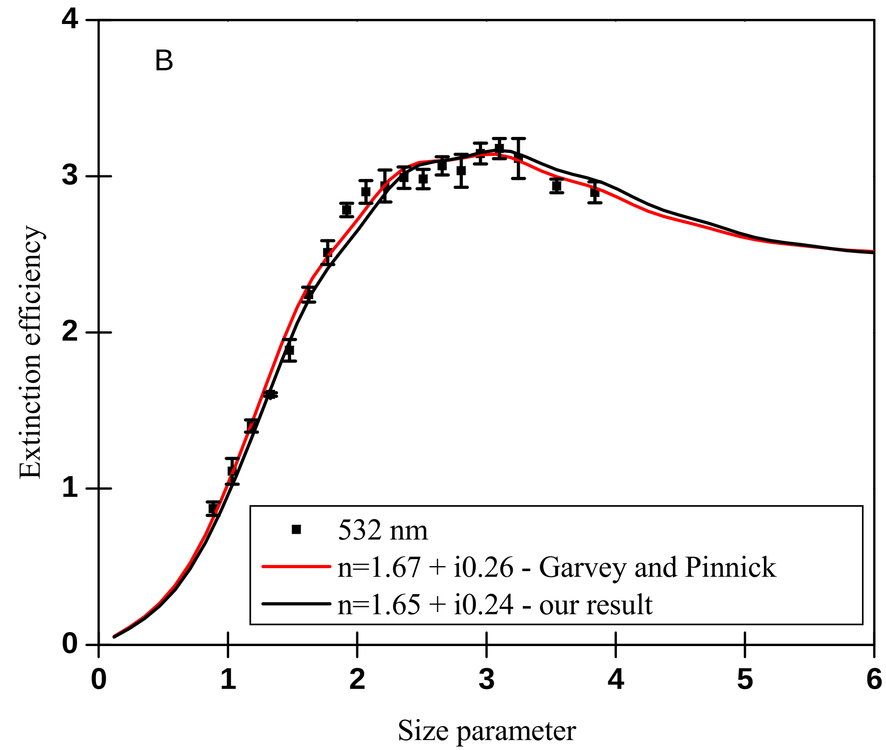

Dinar, Faraday Discuss. 2008

$\alpha = \pi D / \lambda$

Retrieval by Mie ($\lambda \approx d$) calculation – no *a-priori* assumption of refractive index

From presentation by Y. Rudich

Angstrom exponent of HULIS samples: 3 to 5

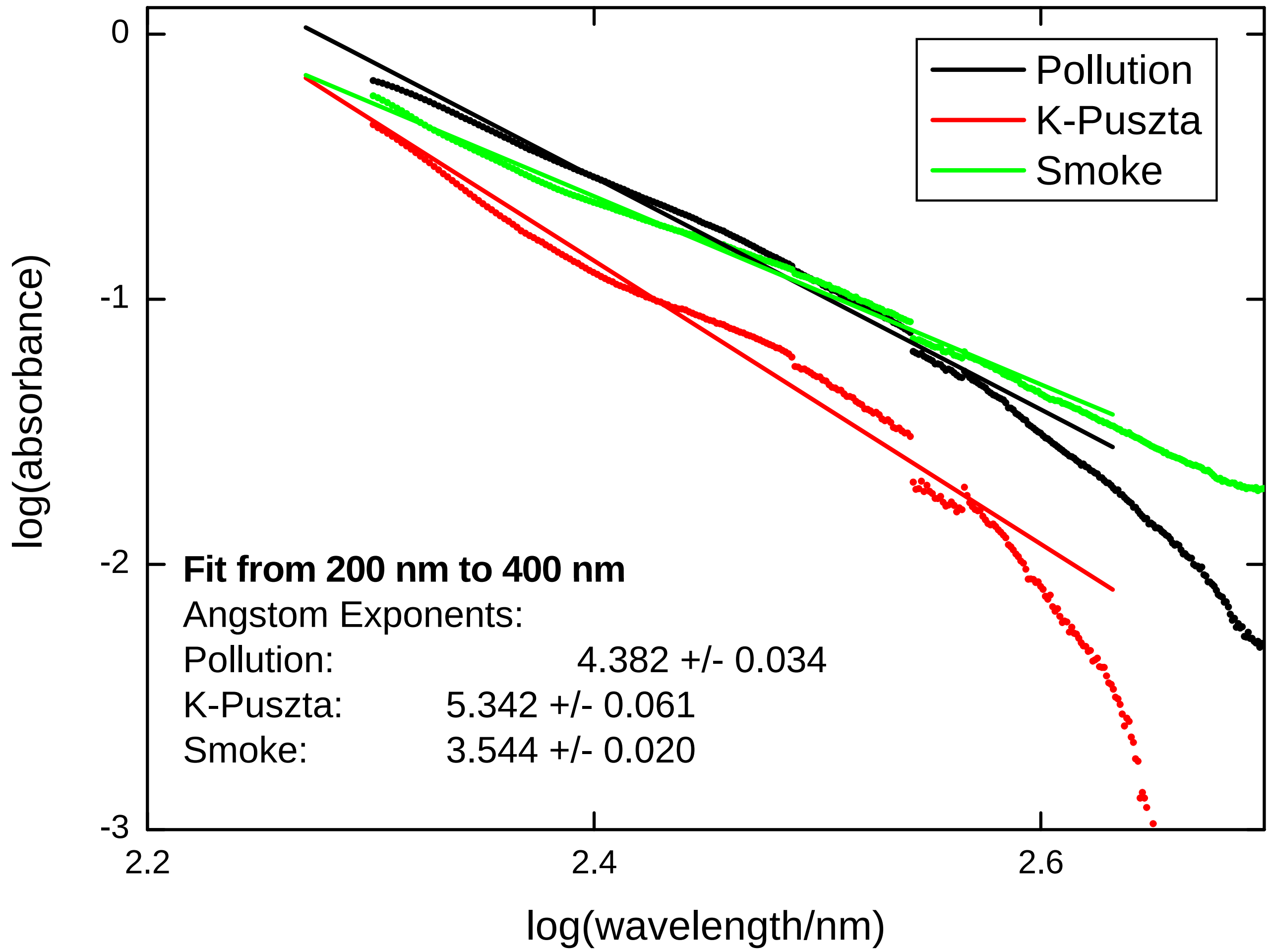

High spectral dependence. Hoffer et. al. measured Å=7 (BB HULIS), Kirchstetter measured Å=2.5 (OC extracts)

From presentation by Y. Rudich

Shape effects on the phase function:

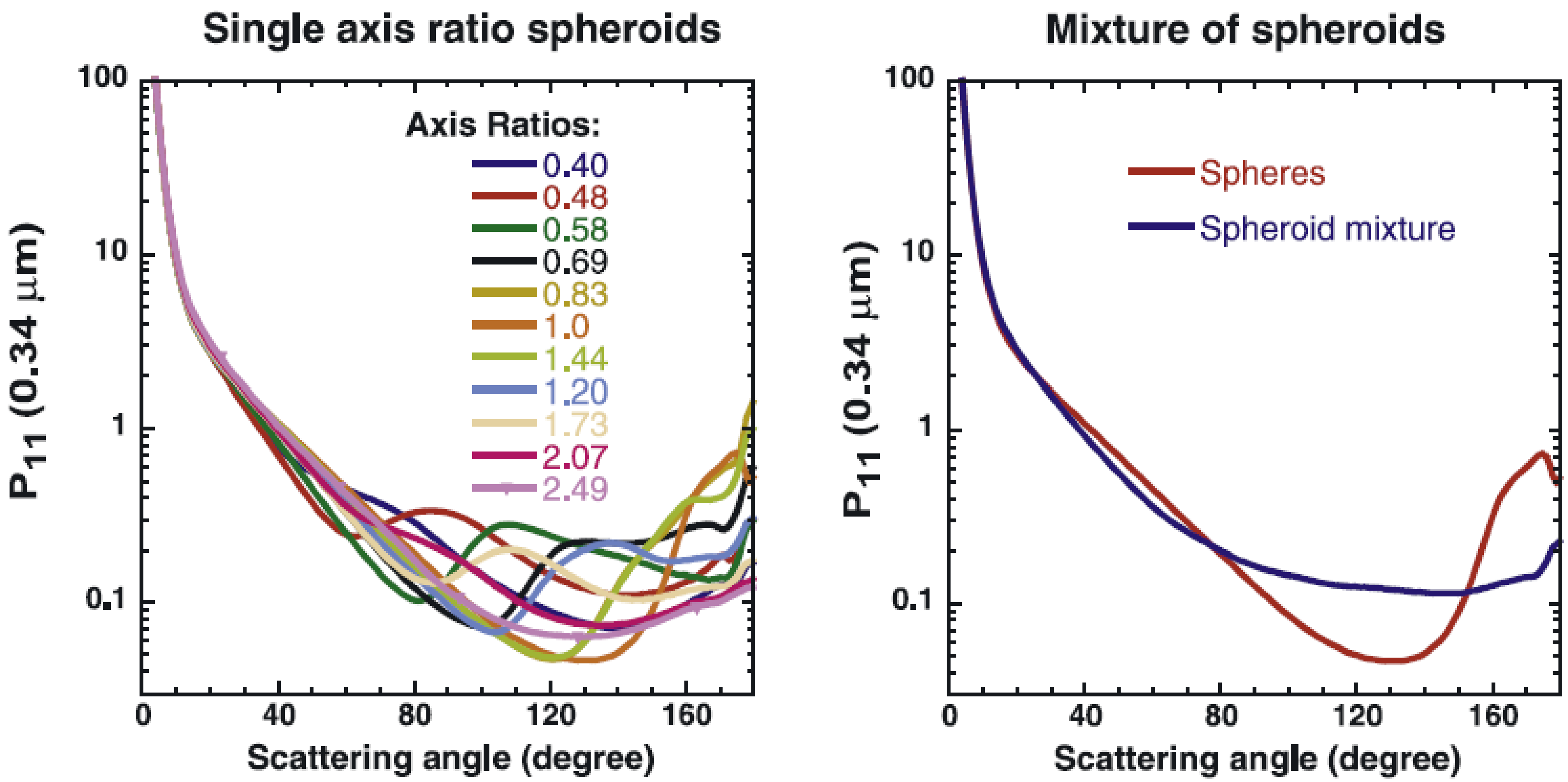

Figure 3. (left) $P_{11}(\Theta, \lambda, \varepsilon_p)$, the phase functions of desert dust simulated for the spheroid model with 11 single axis ratios ε_p. (right) $P_{11}(\Theta, \lambda)$, the phase function of desert dust simulated as a mixture of spheroids with different ε_p (blue line). $P_{11}(\Theta, \lambda)$ is obtained by integrations of $P_{11}(\Theta, \lambda, \varepsilon_p)$ with axis ratio distribution $dn(\varepsilon_p)/d\ln\varepsilon$. Also shown is $P_{11}(\Theta, \lambda)$, the phase function of desert dust simulated under assumption of spherical particles (red line). All phase functions were simulated with the size distribution and complex refractive index of the Saudi Arabia desert dust model [*Dubovik et al.*, 2002a].

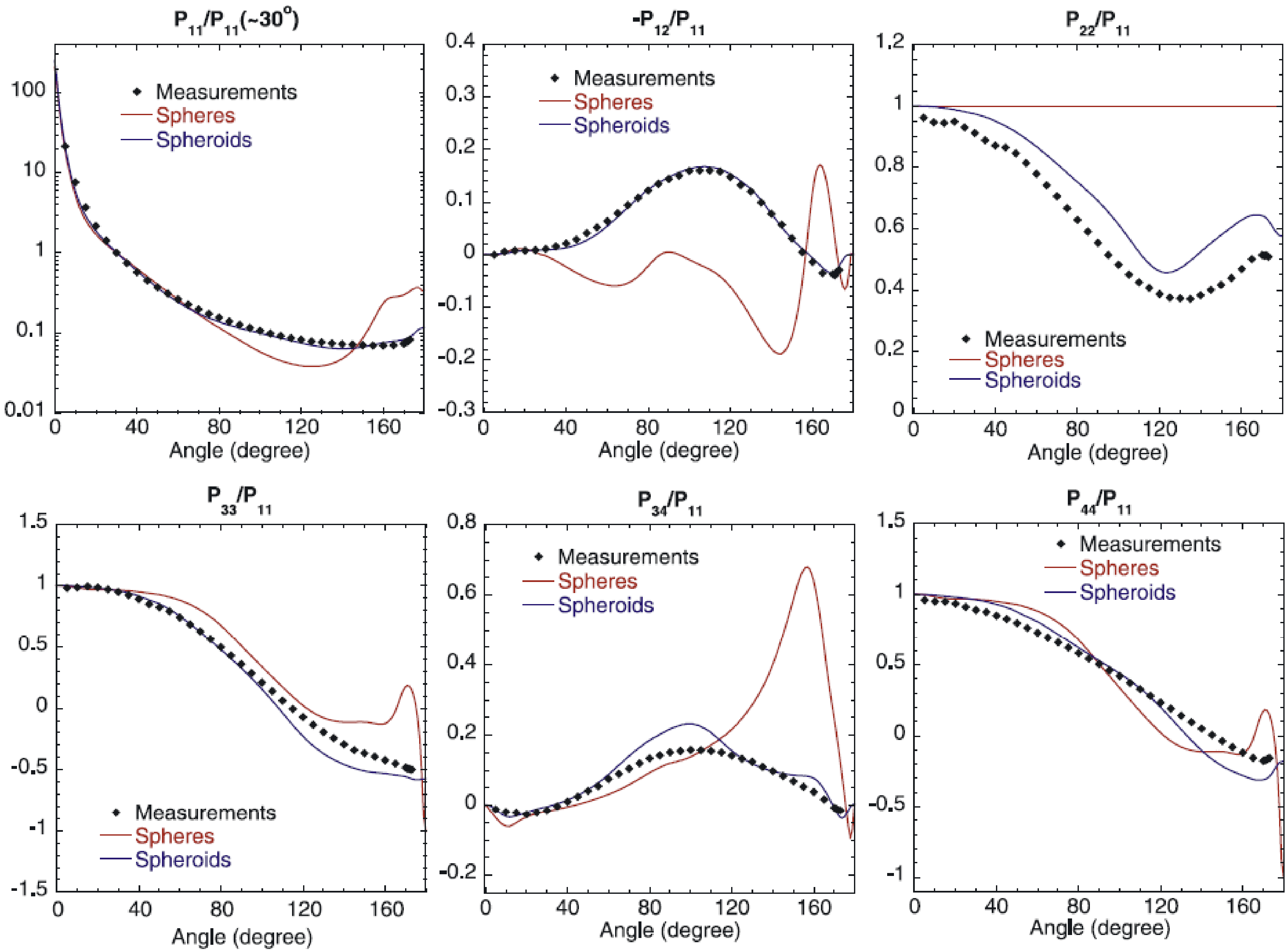

Figure 8. Results of fitting a Feldspar scattering matrix measured at 0.441 μm. The blue line shows the simulation based on the assumption of spheroidal particle shape. The red line shows scattering matrices simulated for spherical particles using the size distribution and complex refractive index retrieved using the spheroid model.

More on aerosols: variation in size , shape and composition:

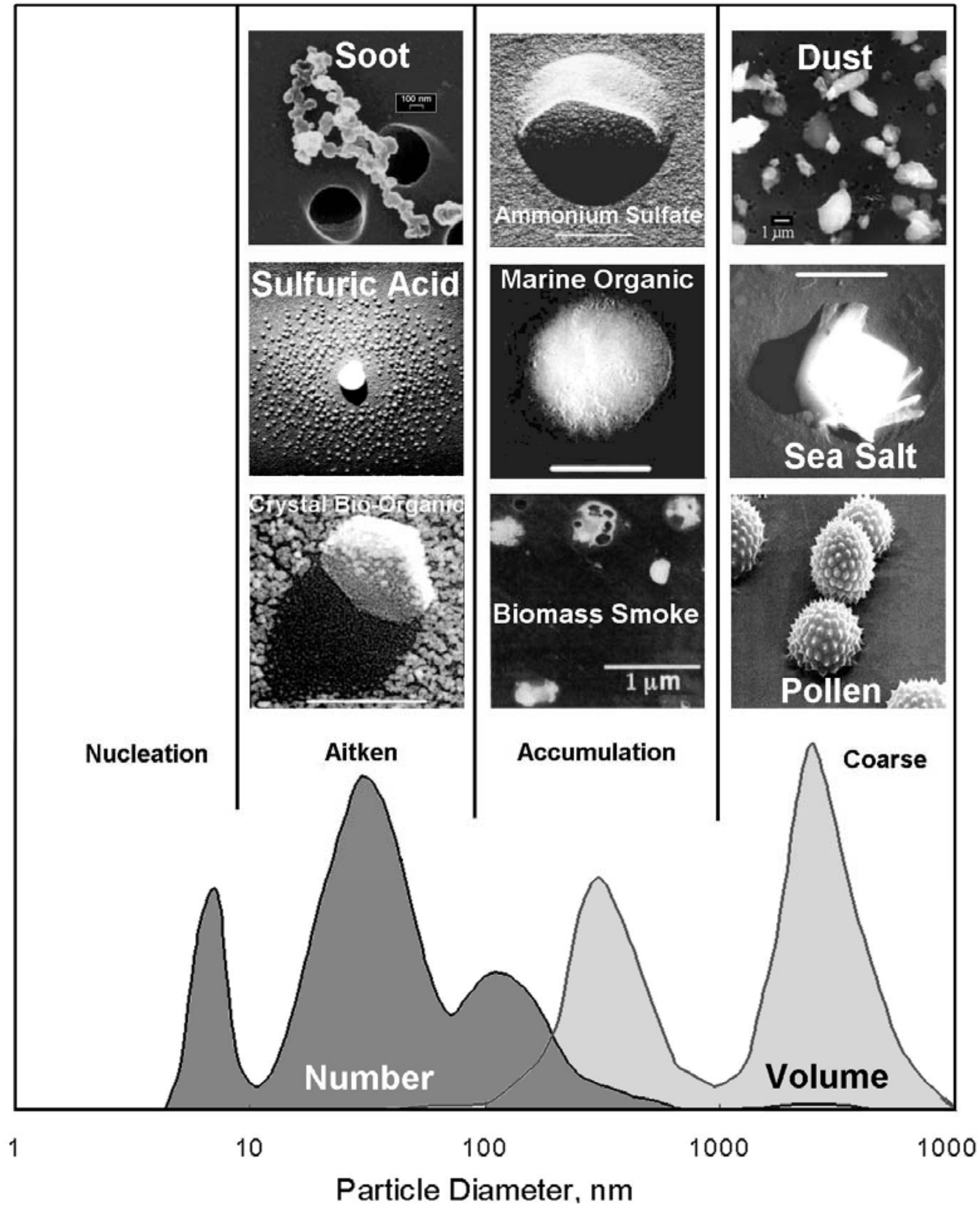

*vista.cira.colostate.edu/improve/Education/Workshops/WESTAR/Malm/**partii_malm**.ppt*

Mass (hence size) distribution of atmospheric particles:

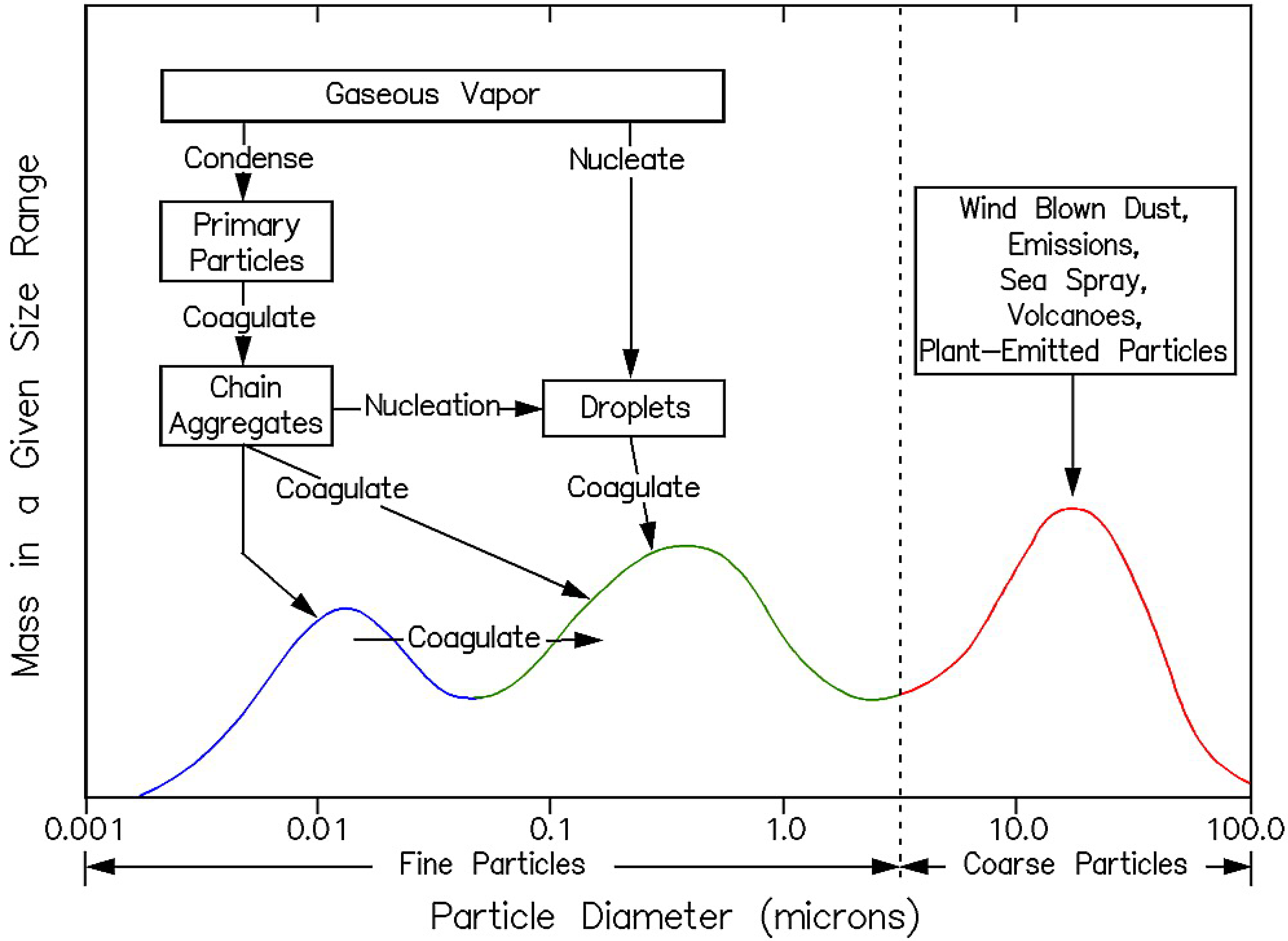

*vista.cira.colostate.edu/improve/Education/Workshops/WESTAR/Malm/**partii_malm**.ppt*

How relative humidity change optical properties of soluble substances – soluble organic material and sea

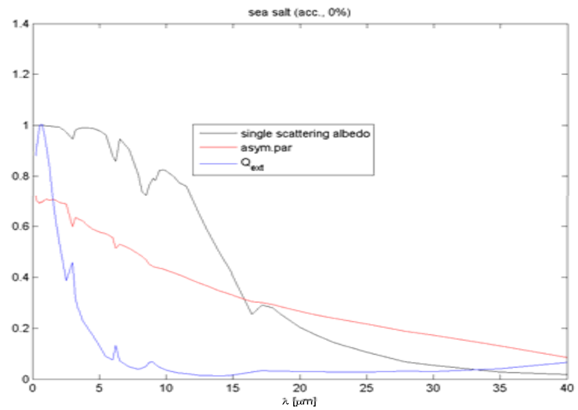

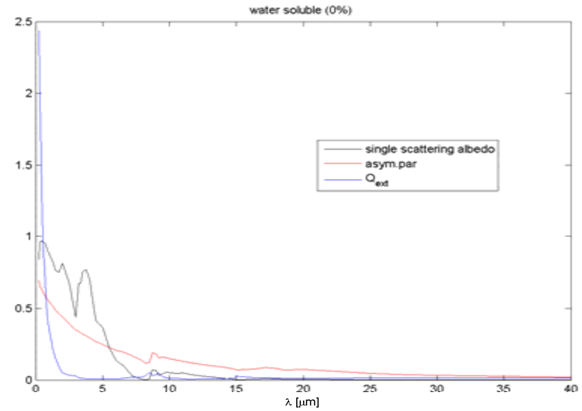

At low relative humidity , organic soluble material has less single scattering albedo ,and higher Qext for shorter wavelengths

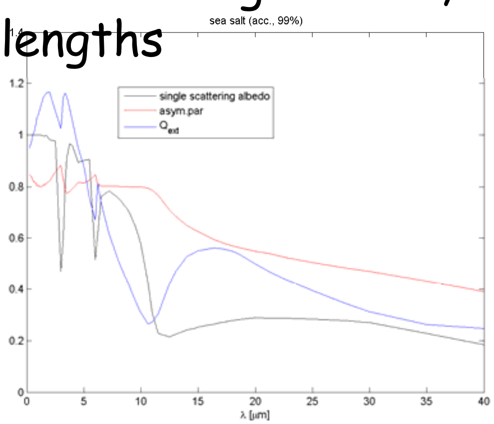

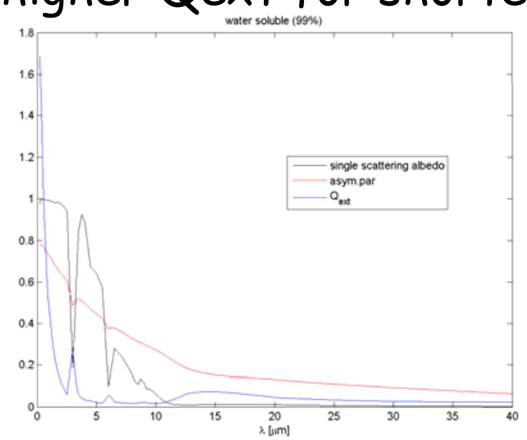

At high relative humidity , organic soluble material have higher volume and more material is dissolved, therefore its properties change.

Continental Common Aerosols

Olga Sima and Ran Vardimon (taken from "OPAC")

Continental and urban aerosol mixtures consist of 3 main aerosol types:
Water soluble (~60%) - sulfates, nitrates and other organic substances
insoluble (~40%) - mostly soil particles with a certain amount of organic material
soot (<1%) - well, soot... (absorbing black carbon)

We compared the <u>attenuation coefficients</u> (normalized per concentration):

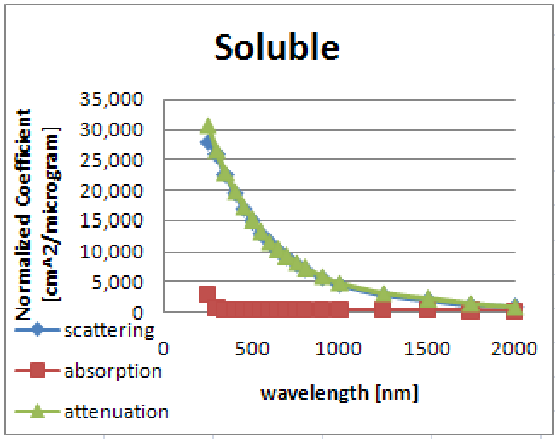

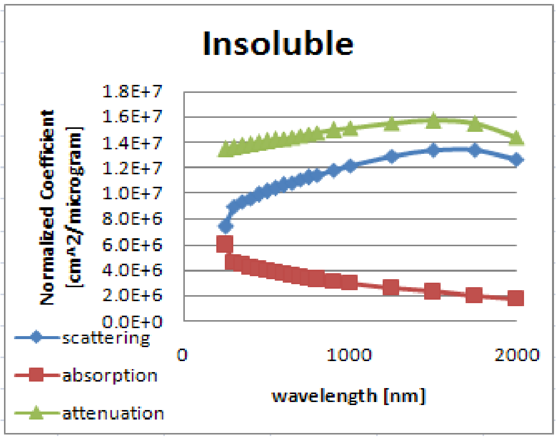

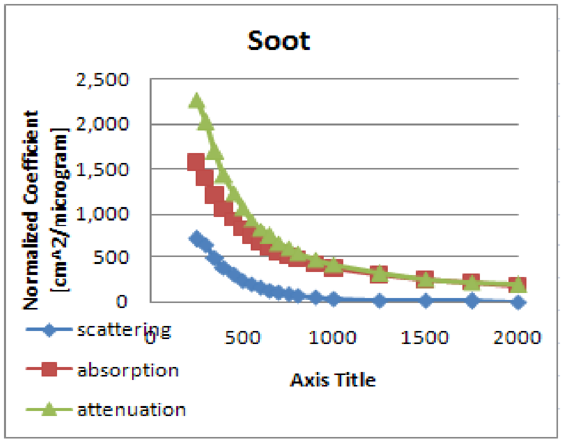

Rmod = 0.03 µm

Rmod = 0.5 µm

Rmod = 0.01 µm

Insoluble particles attenuation is dominant!

All three aerosol types have lognormal size distributions.
Soot (black) has higher absorption coefficient (> scattering).

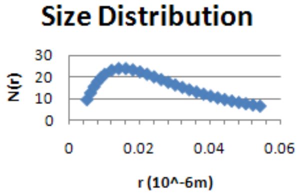

Method: Mie modeling based on microphysical data.

Inverse approaches:

Sunlight changes as it is going through the atmosphere.
Observing the sun directly at specific wavelength provides for atmospheric integrated optical depth → concentration (e.g. water vapor).
Calculations from remote sensing involve two atmospheric passages.

No vertical distribution information.

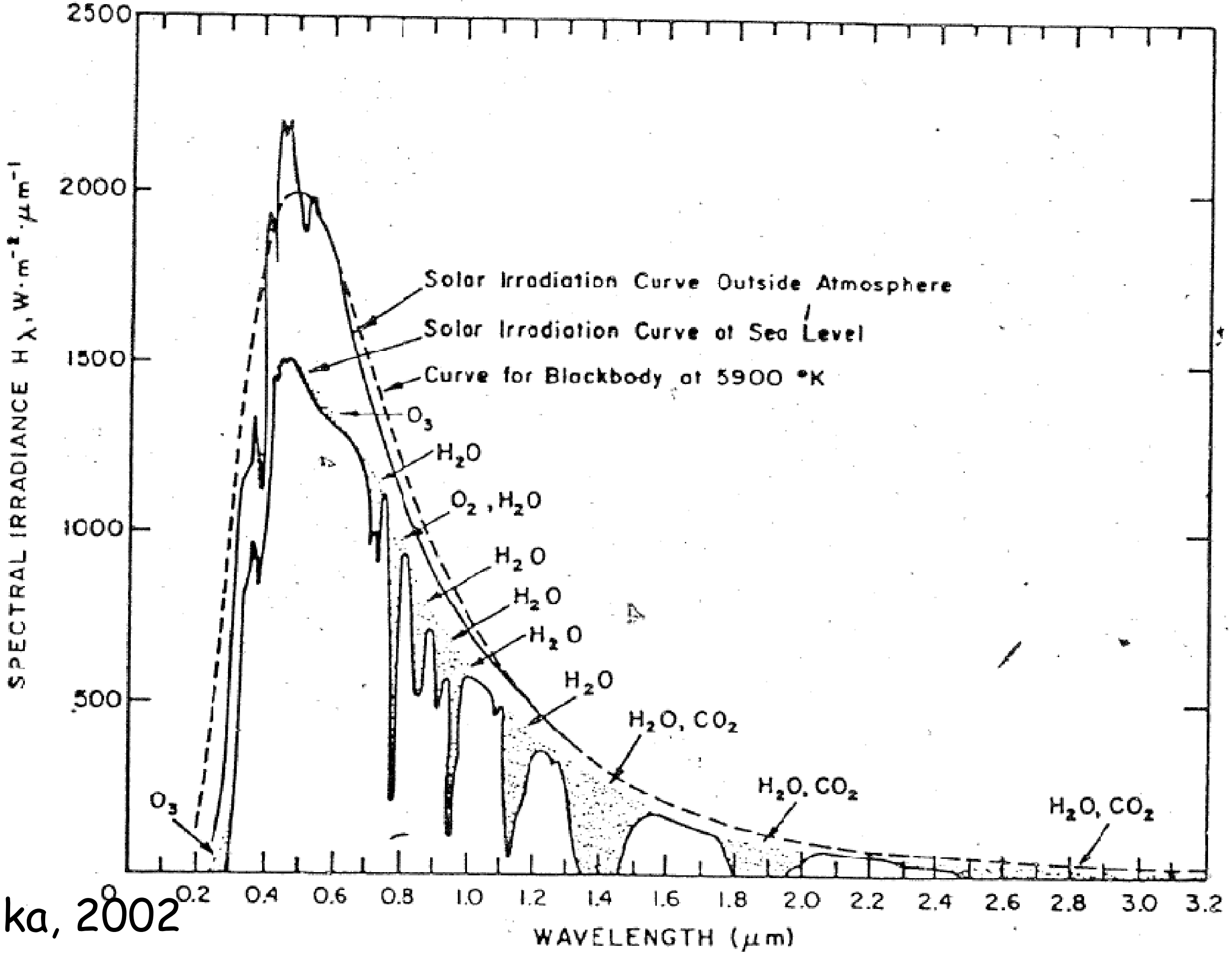

From Kopeika, 2002

AERONET (AErosol RObotic NETwork):

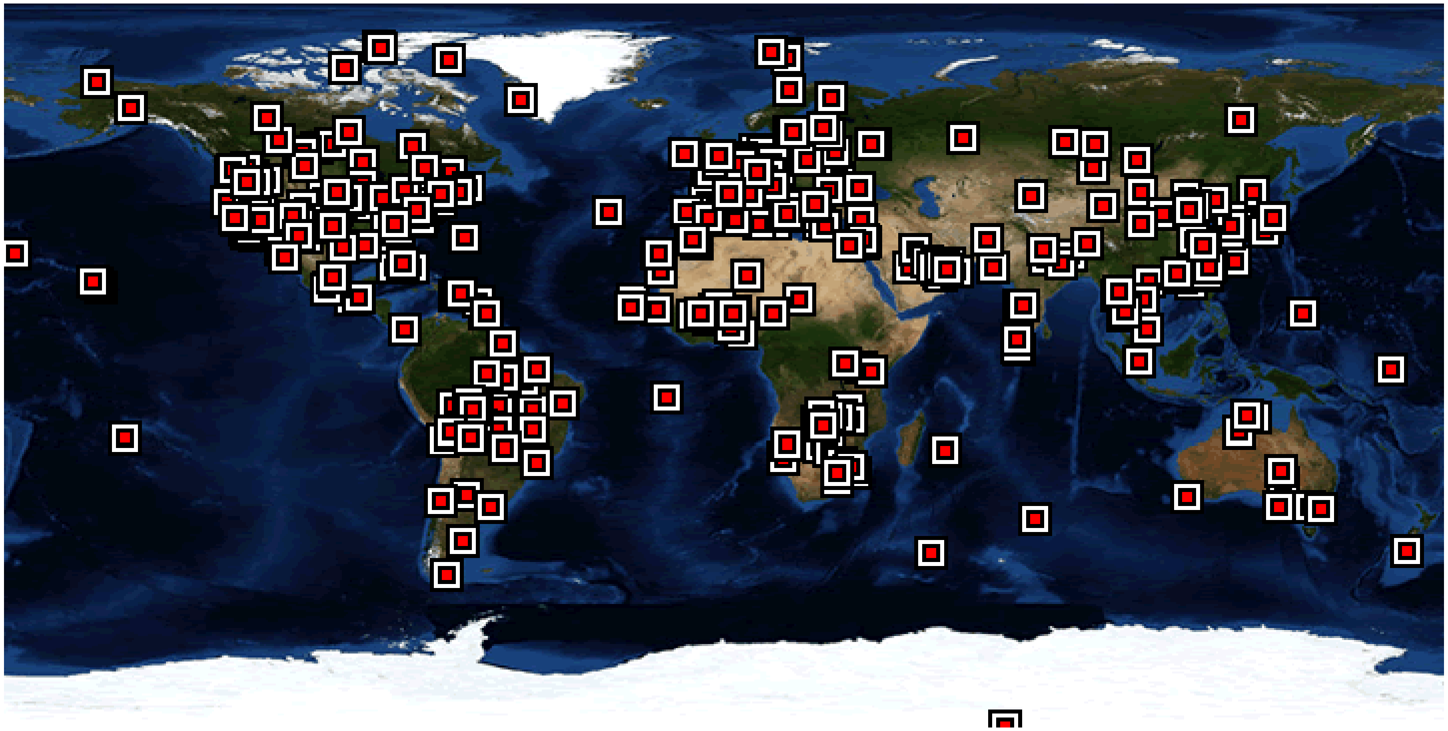

AOD:

Sun photometer measurements of the direct (collimated) solar radiation provide information to calculate the columnar aerosol optical depth (AOD). AOD can be used to compute columnar water vapor (Precipitable Water) and estimate the aerosol size using the Angstrom parameter relationship.

Effect of absorption on transmission:

ATMOSPHERIC TRANSMISSION

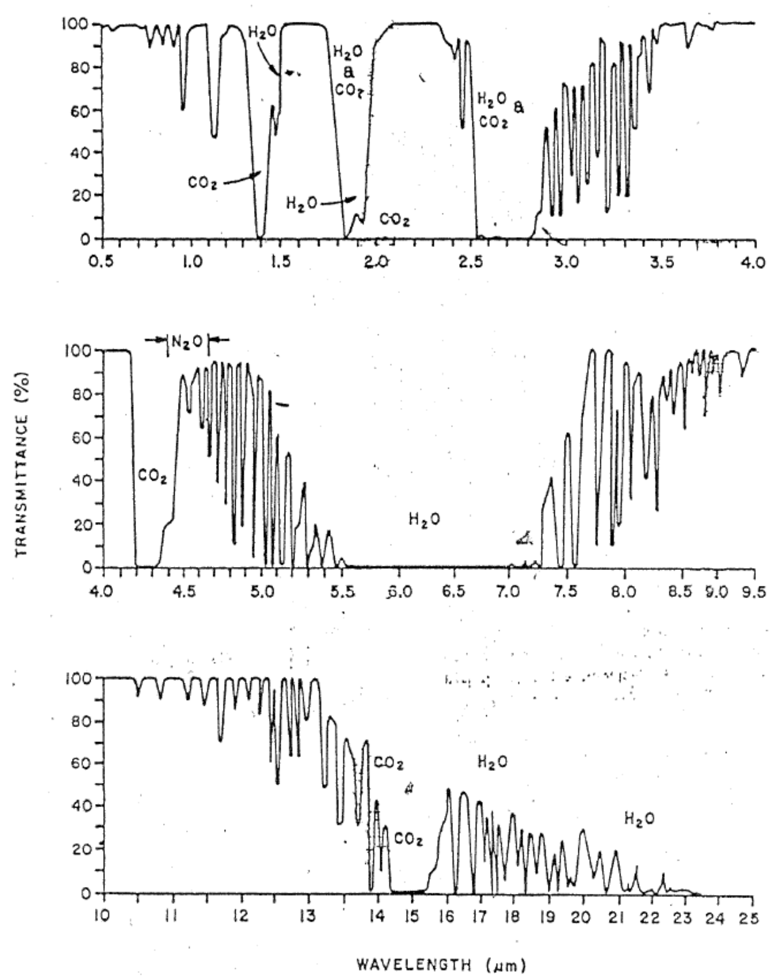

Transmission of 1000 foot horizontal air path at sea level, 5.7 mm precipitable water, 79°F temperature. (Reprinted with permission of Santa Barbara Research Center)

considers absorption but not scattering

From Kopeika, 2002

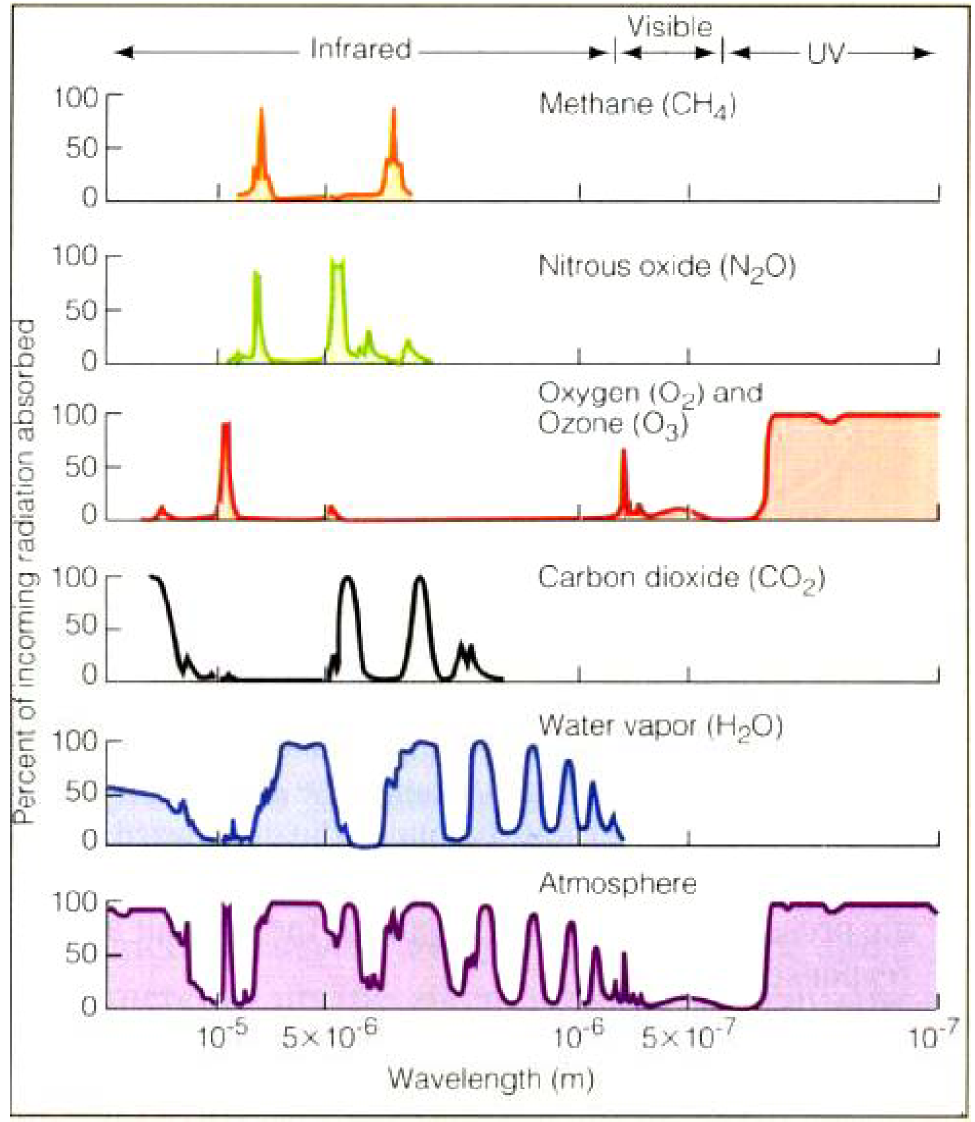

Plot from GEOG-1425 class notes, Katherine Kink, University of Minnesota. Note inverted x-scale.

Almucantar (circle on the celestial sphere parallel to the horizon) measurements:

Measurements of cloud free day angular distribution of sky radiance + AOD + RT calculations are used to obtain:

Particulate size distribution
Index of refraction (real and imaginary)
Spectral single scattering albedo

Requires consideration of three main components:

1. Gaseous absorption (avoided by choice of λ, and use of climatologies).
2. Molecular scattering (calculated for given Pressure).
3. Aerosol absorption and scattering.

Minor (ignored) components: ground albedo, stratification

Figure 8: Cimel performing a GOSUN procedure

Use libraries of single particles optical properties (Mie or other)

Needs: RT model
Optimum inversion scheme

LEVEL 2 Retrievals

Primary Data-base:
- τ Level 2
- All Solar Zenith angles
- 10 symmetrical angles

Filters:
- τ is for Level 2
- Solar Zenith Angle ≥ 25°
- Size Distr. tails < 15% of maximum
- almucantar symmetrical at **21 angles**

Sky fitting error filter:

error: 5%-15%

Check for Non-sphericity

error: < 5%

Filters:

$\tau(440) \geq 0.4$

Solar Zenith Angle ≥ 45°

Level 2 Spherical Aerosol Retrievals:

-Size distribution
(0.05 $\mu m < r < 15 \mu m$)

- Real Part of Ref. Index
- Imaginary Part of Ref. Index
- Single Scattering Albedo
(λ= 0.44; 0.67; 0.87; 1.02 μm)

Level-2 Non-Spherical Aerosol Checks and Processing

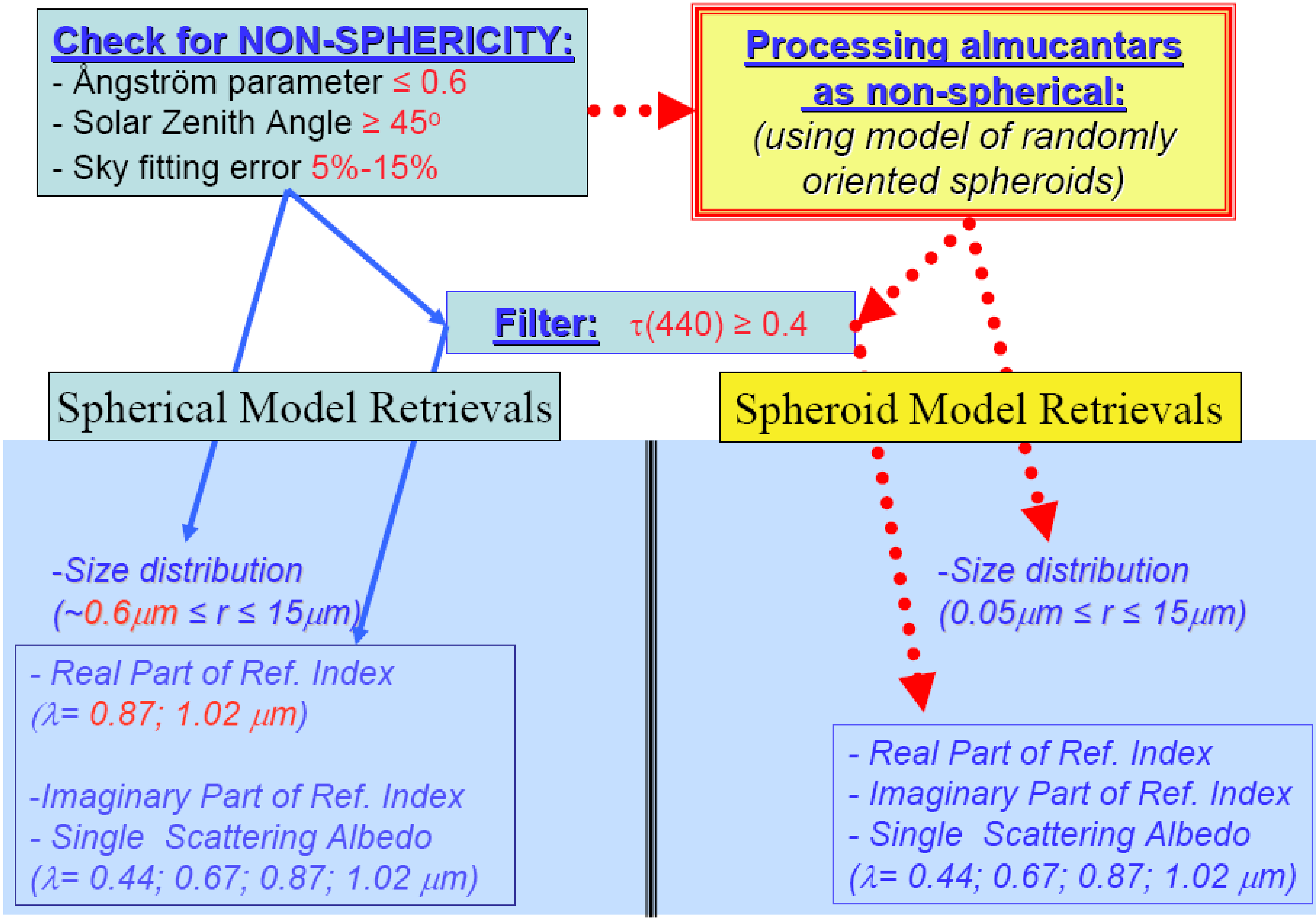

Summary of aerosol optical properties retrieved from worldwide AERONET network of ground-based radiometers.

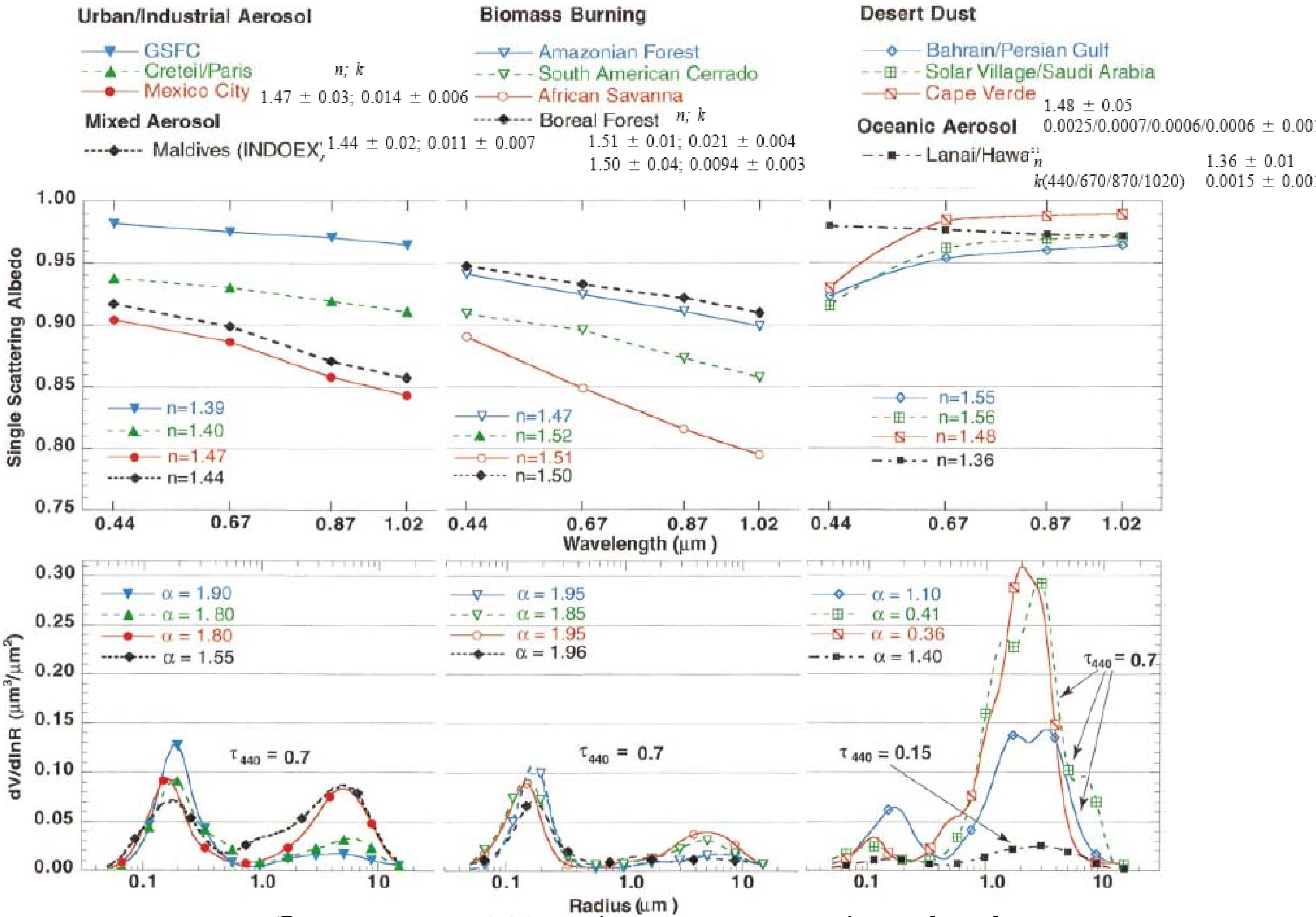

α - Angstrom Exponent at 440 and 870 nm; n - index of refraction

Biomass-Burning Aerosols*

- Biomass-burning in Zambia (savanna) during the dry season (Aug.-Sep.) of 1997
- Measurement done with AERONET
- SSA (ω_0) = 0.82–0.85 (at 550nm)

* Eck et al (2001), *J.G.R.*, **106**, 3425-3448

Size Distribution

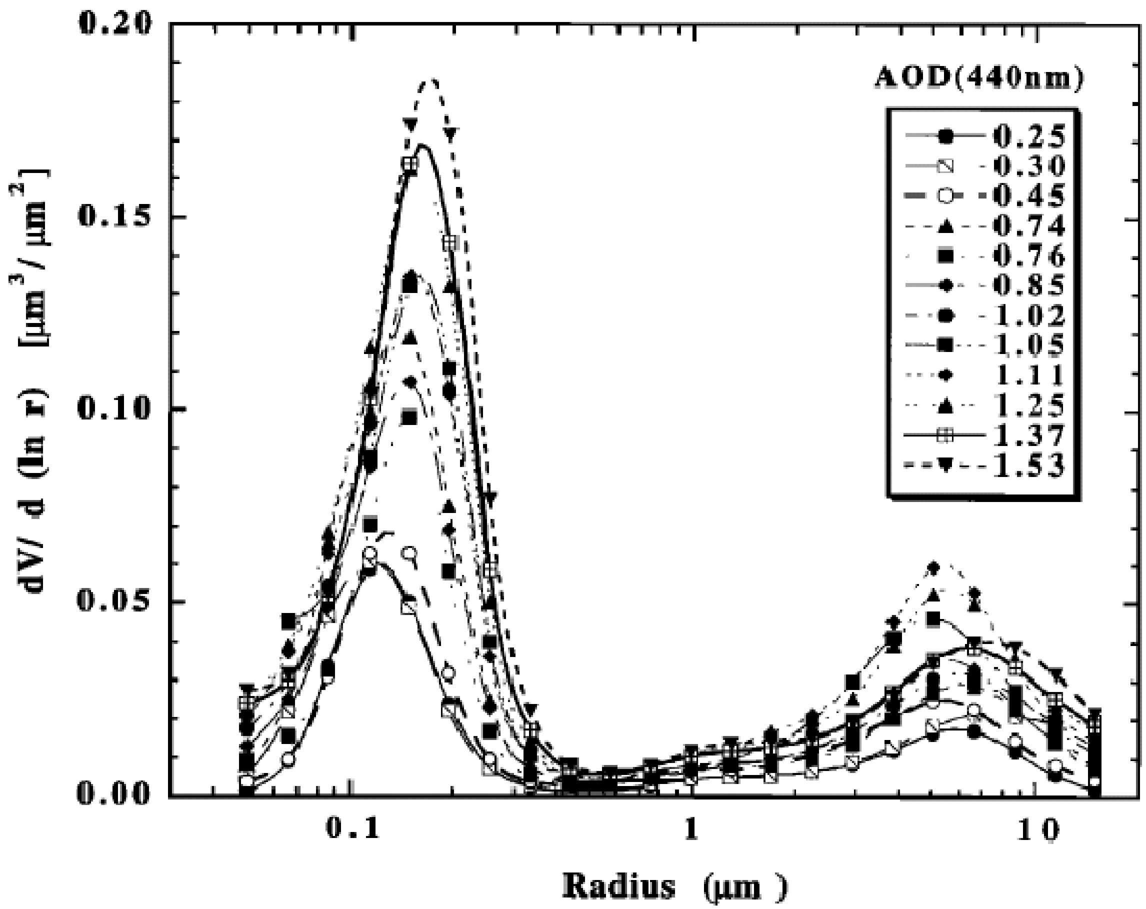

Figure 5. Aerosol volume size distributions for biomass burning aerosols in Mongu, Zambia, for August 25 to September 7, 1997, for aerosol optical depth at 440 nm varying from 0.25 to 1.53. Aerosol size distribution retrievals were derived from simultaneous analysis of sky radiances in the almucantar and spectral τ_a at 440, 675, 870, and 1020 nm.

Single Scattering Albedo

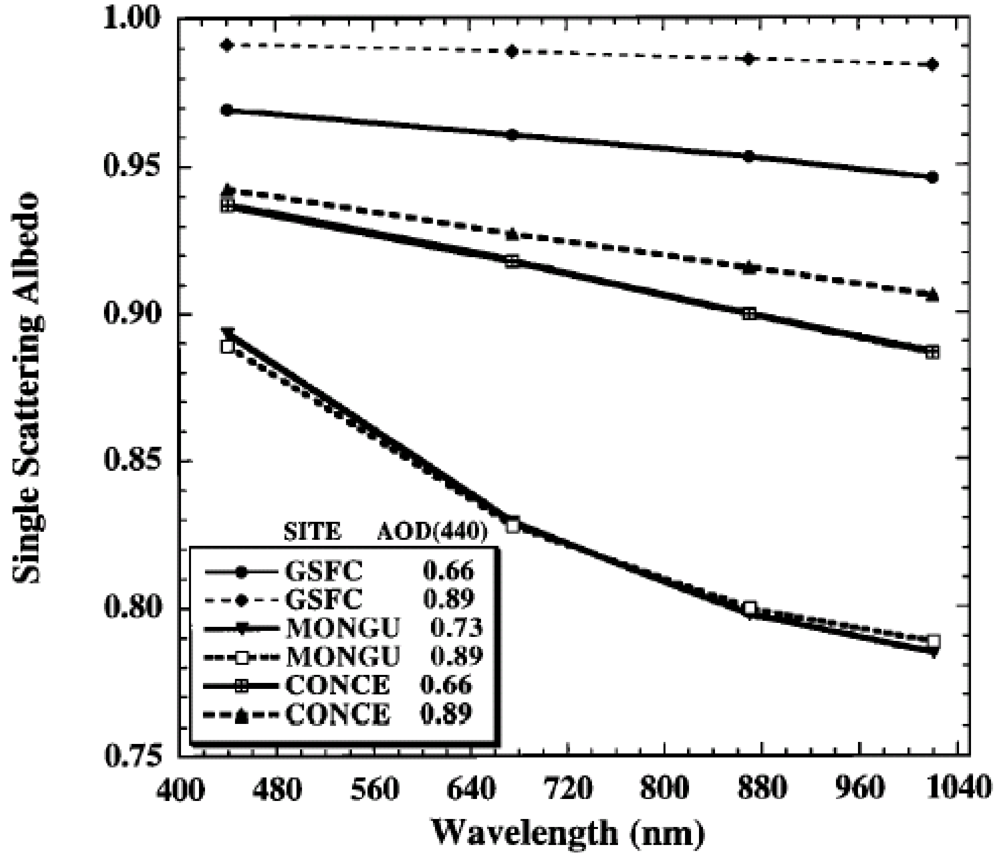

Figure 10. Comparison of spectral (440 to 1020 nm) ω_0 retrievals made with AERONET radiometers at three sites, for τ_a at 440 nm ranging from 0.66 to 0.89. The sites are Mongu, Zambia, with savanna burning smoke, Concepcion, Bolivia, with pasture/forest burning smoke in Amazonia, and Goddard Space Flight Center, Maryland, with urban/industrial pollution. See Figure 6 for a comparison of the aerosol volume size distribution for these same sites.

Emission spectra is also affected by aerosols:

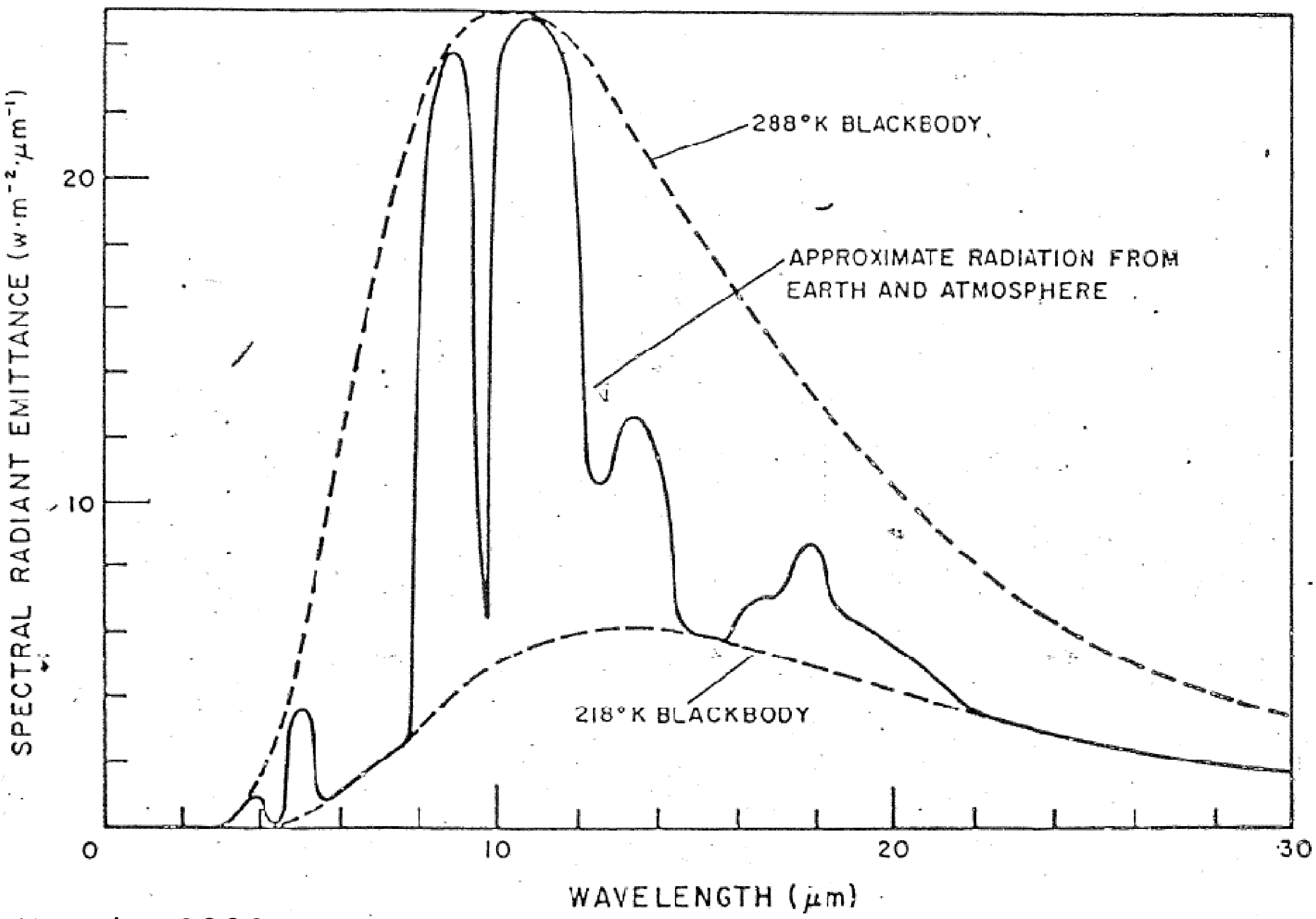

From Kopeika, 2002

Conclusions

1. Atmospheric OP are complex

2. Creative approaches provide possibility to retrieve AOPs from routine observations.

3. Need for validation (laboratory work is critical).

4. Much work is left for the next generation to tease out (e.g. 'anomalous' absorption, absorption by clouds).